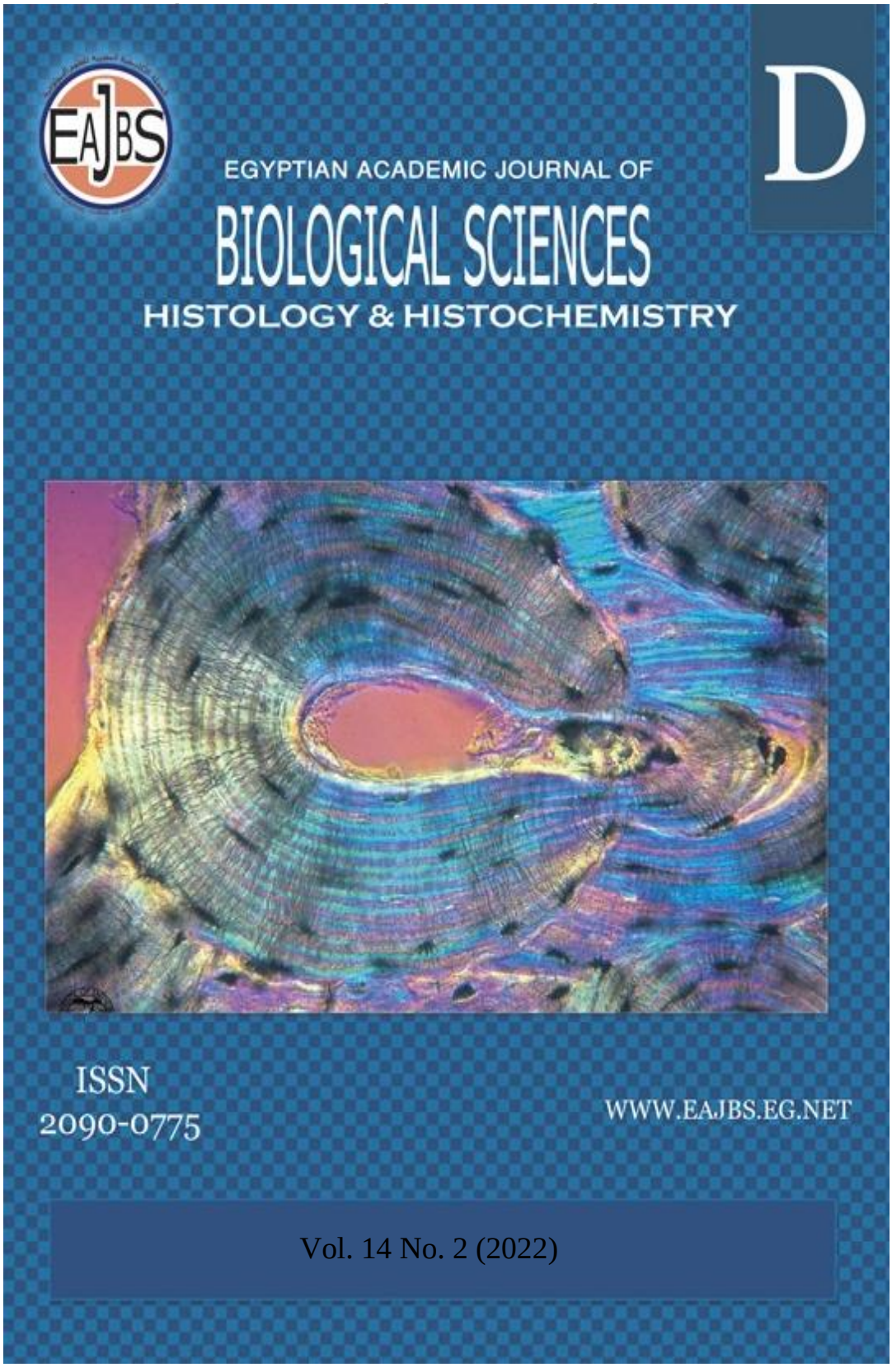

Citation: Egypt. *Acad. J. Biolog. Sci. (D-Histology and histochemistry) Vol.14(2) pp181-199(2022)*
DOI: 10.21608/EAJBSD.2022.276324

Egypt. Acad. J. Biolog. Sci., 14(2): 181-199 (2022)

Egyptian Academic Journal of Biological Sciences
D. Histology & Histochemistry
ISSN 2090 – 0775
http://eajbsd.journals.ekb.eg

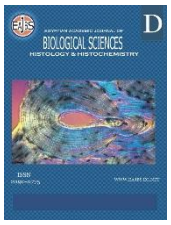

Effect of Amiodarone on Thyroid Gland in Adult Male Albino Rats: A Histological and Immunohistochemical study

Nourhan Mahmoud El-Sayed, Khaled Naiem Hamdy, Ahmed Yehia Moustafa, Hagar Yousry Sayed Rady and Ahmed Samir Sadek
Anatomy & Embryology Department, Faculty of Medicine, Ain Shams University, Cairo, Egypt.
E.Mail*: dr_ahmedsamir@med.asu.edu.eg

ARTICLE INFO
Article History
Received:14/9/2022
Accepted:17/11/2022
Available:21/11/2022

***Keywords*:**
Amiodarone – Thyroid - Caspase III.- Rat.

ABSTRACT

Background: Amiodarone (AMD) is a benzofuran derivative, used in the management of angina and refractory ventricular arrhythmia. AMD may lead to either hypothyroidism or hyperthyroidism, depending on the daily dietary allowance of iodine. **Aim of the Work:** The aim of the current study is to investigate the structural and biochemical changes of the thyroid gland of adult male albino rats after exposure to different doses of AMD. **Material and Methods:** Thirty adult male albino rats were used in the experiment, they were divided into three groups; the Control group (Group I, N=10); AMD therapeutic dose-treated group (Group II, N=10), received AMD at a dose of 30 mg/Kg daily for 12 weeks by oral gavage; AMD toxic dose-treated group (Group III, N=10), received AMD at a dose of 60 mg/Kg daily for six weeks by oral gavage. At the end of the experiment, blood samples were taken from rats to estimate the serum concentration of tri-iodothyronine (T3), thyroxine (T4), and thyrotrophin (TSH). The thyroid glands of all rats were removed, and specimens from the glands were prepared and processed for histological examination under a light microscope. An immunohistochemical study was conducted using Caspase III. **Results:** Biochemical examination revealed a highly significant increase of serum T3 and T4, with Concomitant suppression of TSH. Histopathological examination of thyroid tissues from AMD therapeutic dose group (Group II) showed marked evidence of thyrotoxicosis in the form of microcystic follicular changes and peripheral scalloping, cellular degeneration with scanty cytoplasm and vesicular nuclei appeared. These changes became more severe in AMD toxic dose group (Group III) in the form of epithelial hyperplasia with atypical nuclear features, together with thyroid tissue damage with hemorrhage and necrosis. **Conclusion**: Amiodarone had detrimental effects on the rat's thyroid tissue when administered either in therapeutic or toxic doses.

INTRODUCTION

The thyroid gland lies in the lower neck opposite C5 to T1 vertebrae and is composed of two lobes connected by an isthmus in the midline (Branca, *et al.*, 2022). Its primary function is to produce thyroid hormones; tri-iodothyronine (T_3), thyroxin (T_4) and the peptide hormone calcitonin (Singh, 2020). The thyroid hormones greatly affect the human body concerning metabolism.

They increase the basal metabolic rate and affect almost all body tissues, appetite, absorption of substances, and gut motility (Talat, *et al.,* 2019).

AMD is the drug of choice in most cases of arrhythmia. Although it is considered a class III antiarrhythmic drug, it has also class I, class II, and class IV pathways (Jabrocka-Hybel, *et al.,* 2015). AMD is used to manage variable cases of arrhythmia like supraventricular and ventricular tachyarrhythmias (Benvenga, *et al.,* 2018). AMD is a benzofuran compound composed of 37% iodine by molecular weight, so it releases a 20 to 40 folds higher iodine level compared to its daily body requirements (Fischer, *et al.,* 2022). However, the lipophilic property and long half-life of AMD led to an increase in its concentration in many tissues causing several hazardous effects such as; photosensitivity, corneal micro-deposits, pulmonary and hepatic toxicity, peripheral neuropathy, thyroid dysfunction (Epstein, *et al.,* 2016). AMD might lead to either hypothyroidism or hyperthyroidism, depending on the daily dietary allowance of iodine (Nafrialdi, *et al.,* 2016). Also, due to the nearly similar structure of AMD and thyroid hormones, AMD can act on many cell types and organs including the liver and pituitary gland as a thyroid hormone reducing thyroid hormones uptake by these tissues (January, *et al.,* 2014).

The aim of the current study is to investigate the structural and biochemical changes in the thyroid gland of adult male albino rats after exposure to different doses of AMD.

MATERIALS AND METHODS

Experimental Animals:

Thirty adult male albino rats of the Sprague Dawley strain aged 5–6 months old, with an average body weight of 200-250 gm were used in this study. The study was conducted at the Animal House of the Faculty of Medicine, Ain Shams University, according to the guidelines for the care and use of laboratory animals. Rats were housed in polycarbonate cages (4 rats/cage) in a constant temperature (22-24°C) and light-controlled room on an alternating 12:12 h light-dark cycle and had free access to food and water. Rats were kept for one week before beginning the experiment for acclimatization. The Health Research Ethics Committee, Faculty of Medicine, Ain Shams University, Egypt (Code: FMASU/ MS/31/2022) approved the study protocol.

Drugs:

1- Amiodarone, is available as tablets 200mg Amiodarone HCL "Cordarone®" Sanofi Aventis, Cairo, Egypt.

2- Saline 0.9% is available as a pack 500ML, Otsuka, Cairo, Egypt

Experimental Design:

Animals were randomly divided into three groups (Each group consisted of 10 rats).

•**Group I**: (Control Group) was divided into two sub-groups; 1-Group Ia: Five rats received no treatment and received only distilled water by oral gavage, and Group Ib: Five rats received 3ml of 0.6% methylcellulose orally by oral gavage.

•**Group II**: (AMD therapeutic dose-treated group) 10 rats received AMD in a daily dose of 30 mg/kg body weight dissolved in 3 ml of 0.6% methylcellulose for 12 weeks by oral gavage (Zidan, 2011).

•**Group III**: (AMD toxic dose-treated group):10 rats received amiodarone in a daily dose of 60 mg/kg body weight dissolved in 3 ml of 0.6% methylcellulose for six weeks by oral gavage (El Sayed, *et al.,* 2007).

At the end of the experiment, all rats were sacrificed on the planned days by a lethal dose of anesthesia according to the protocol of the Animal Care at Ain Shams University. Blood samples were taken from rats just prior to sacrifice to estimate the serum concentration of tri-iodothyronine (T3), thyroxine (T4), thyrotrophin (TSH). The thyroid gland was placed in a 10% neutral-buffered

formalin solution for one week, and then processed to paraffin blocks. 5 µm paraffin sections were used for histopathological examination under a light microscope using Hematoxylin and Eosin (Hx & E) and Masson 's trichrome (Bancroft and Gamble, 2002). An immunohistochemical study was conducted for the detection of apoptotic thyroid cells using caspase III antibodies (Di Matola, 2000).

Biochemical Measurements:

Rats were anesthetized, and blood samples were taken just prior to the sacrifice of the rats from the retrobulbar venous plexus in a sterile centrifuge tube. The sample was kept at −20°C until the samples will be centrifuged for separation of the sera. The serum T3, T4, and TSH levels were measured (Aslan, *et al.*, 2009).

Morphometric Study & Image Analysis:

NIH "Image J" computer image analysis software version 1.40g was used to measure the following parameters:

- The area percentage of collagen fibers deposition per microscopic field in Masson's trichrome stained sections .
- The area percentage of caspase III immunoreactivities in immune-stained sections .

Calibration of the software was done for each microscopic magnification in order to translate pixels into micrometers. This was done with the aid of a stage micrometer. The area to be measured is masked by the primary mask by adjusting the color threshold. The number of pixels in the mask is divided by the number of pixels of the microscopic field to get the area percentage.

Statistical Analysis:

The collected data were analyzed using a statistical analysis system. Data were presented by mean and standard deviation. One-way ANOVA followed by posthoc Bonferroni test was used to compare the studied three groups of rats according to collagen fiber deposition and the intensity of Caspase III immune reactions. The significance of the data was determined by P-value ($P < 0.05$ or equal to 0.05 was considered significant and $P < 0.001$ or equal to 0.001 was considered highly significant) (Sawilowsky, 2005).

RESULTS

Biochemical Results:

Statistical analysis of thyroid hormone levels showed that there was a statistically significant increase in the levels of T3 and T4 and a statistically significant decrease in the level of TSH in the therapeutic dose-treated group (Group II). Whereas in the toxic dose-treated group (Group III), there was a highly statistically significant increase in the levels of T4 and free T3 and a highly statistically significant decrease in the level of TSH (Table 1 & Chart 1).

Table 1: The mean levels of thyroid gland hormones.

Groups	T3			T4			TSH		
	Mean	SD	P value	Mean	SD	P value	Mean	SD	P value
Control group (I)	4.095	0.584935894		4.916666667	0.24832774		2.603333333	0.311234103	
Therapeutic dose-treated group (II)	6.45	1.243784547	P1= (0.001837583)	6.666666667	1.182652386	P2= (0.005292729)	1.865	0.25913317	P3= (0.001205534)
Toxic dose-treated group (III)	101	1.768615278	P4= (2.17469E-17)	129.0166667	2.104677331	P5= (6.66094E-18)	0.843333333	0.0665332	P6 = (9.27804E-08)

(P) 1 = A significant increase compared to the control group.
(P) 2 = A significant increase compared to the control group.
(P) 3 = A significant decrease compared to the control group.
(P) 4 = A highly significant increase compared to the control group.
(P) 5 = A highly significant increase compared to the control group.
(P) 6 = A highly significant decrease compared to the control group.
SD: Standard deviation.

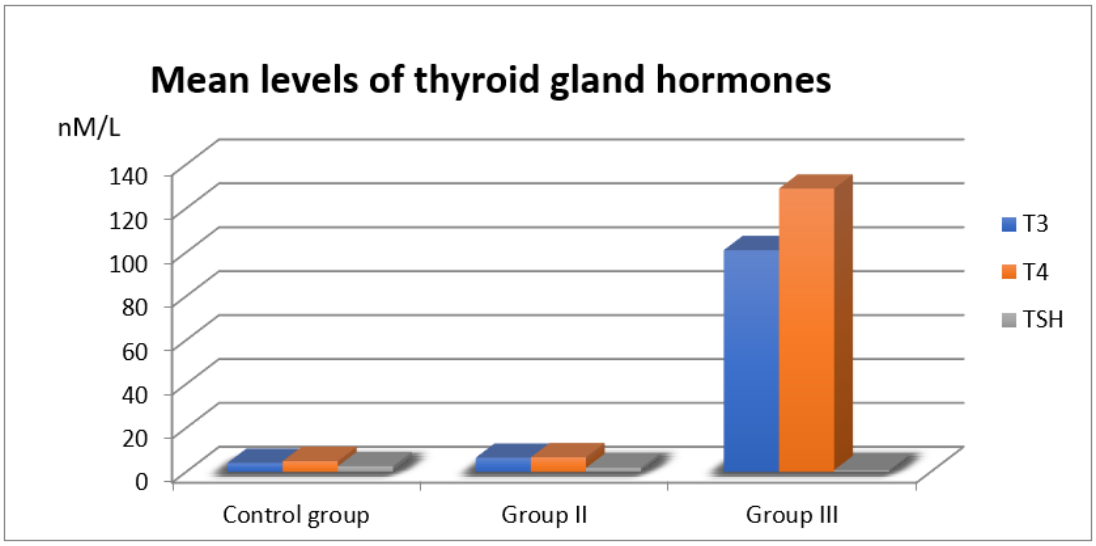

Chart 1: The mean levels of thyroid gland hormones of all groups.

Histological Results*:*

Light microscopic examination of the thyroid glands of rats of group I (control group) showed that the gland is formed of multiple lobules separated by thin connective tissue septa. The thyroid lobule consisted of variable-sized rounded or oval follicles with connective tissue in between. The peripheral follicles were relatively larger than the central ones. Moreover, there was a fine fibrous capsule surrounding the gland (Fig. 1). The follicular lumen was filled with homogenous acidophilic colloids that had peripheral small vacuoles. Parafollicular cells were observed in between the follicles (Fig. 2). Each follicle was lined with a single layer of cuboidal thyrocytes that contain central rounded nuclei. Parafollicular cells were present between the follicles, and blood vessels were seen in between the lobules. Each follicle was surrounded by a thin basement membrane having spindle-shaped fibroblasts with flattened nuclei (Fig. 3).

Masson's trichrome-stained sections revealed a normal distribution of collagen fibers deposition in the septa between the follicles (Fig. 4).

Immunohistochemical stained sections for caspase III showed weak positive immunoreactivity which appeared as fine brownish granules in the nuclei and the cytoplasm of a few follicular cells (Fig. 5).

Light microscopic examination of the thyroid glands of rats of group II (therapeutic dose treated group) showed moderate loss of normal architecture of the thyroid gland. The acini showed irregularly shaped and sized follicles with micro-cystic follicles (Fig. 6). Thyroid follicles were filled with vacuolated colloids. There was an apparent increase in the number of parafollicular cells in between the follicles. (Fig. 7). Follicles became lined with columnar thyrocytes with vacuolated cytoplasm. The colloid of some follicles showed vacuolations and others showed peripheral scalloping (Fig. 8).

Masson's trichrome stained sections revealed a statistically highly significant increase in collagen fibers deposition in between the follicles compared to the control group (Fig. 9) & (Table 2 & chart 2).

Immunohistochemically stained sections for caspase III showed a statistically significant increase in the nuclear and cytoplasmic immunoreactivity for caspase-3 in many follicular cells as compared to the control group (Fig. 10) & (Table 3 & chart 3).

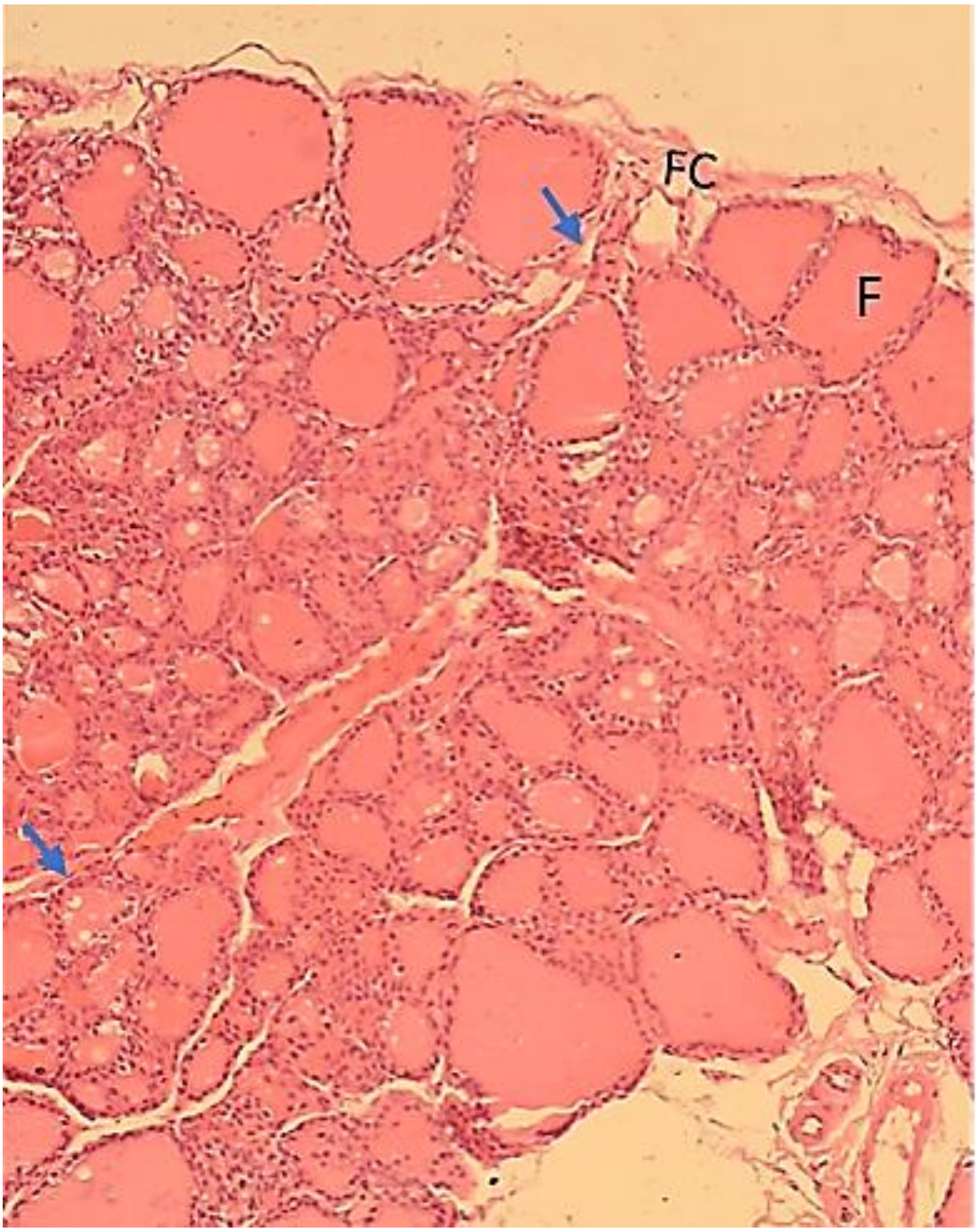

Fig. 1: A photomicrograph of a section of the thyroid gland of rats of GI showing the normal architecture of the thyroid gland, composed of lobules consisting of variable-sized follicles **(F)**, with normal septa **(arrow)** in between the lobules. Notice the fine fibrous capsule **(FC)** surrounding the gland. **(H&E X 100)**

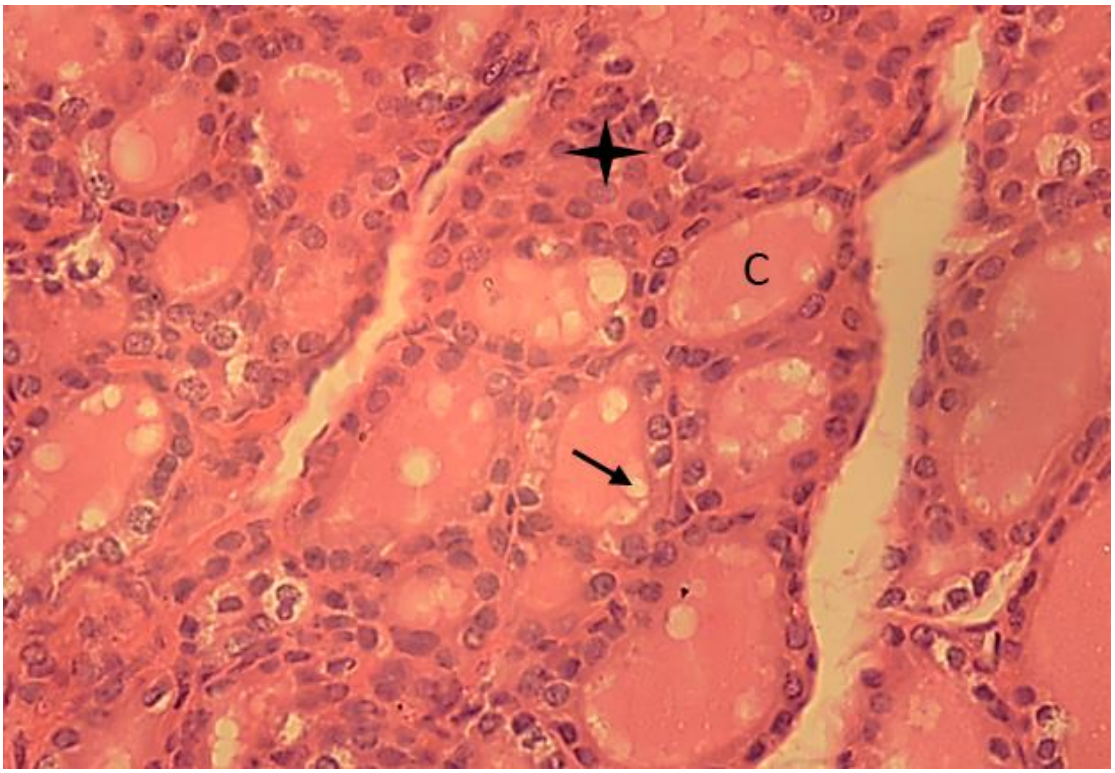

Fig. 2: A photomicrograph of a section of the thyroid gland of rats of GI showing the homogenous acidophilic colloid **(C)** inside the follicular lumina with some normal peripheral small vacuoles **(arrow).** Notice the parafollicular cells in between the follicles **(star).** **(H&E X 400)**

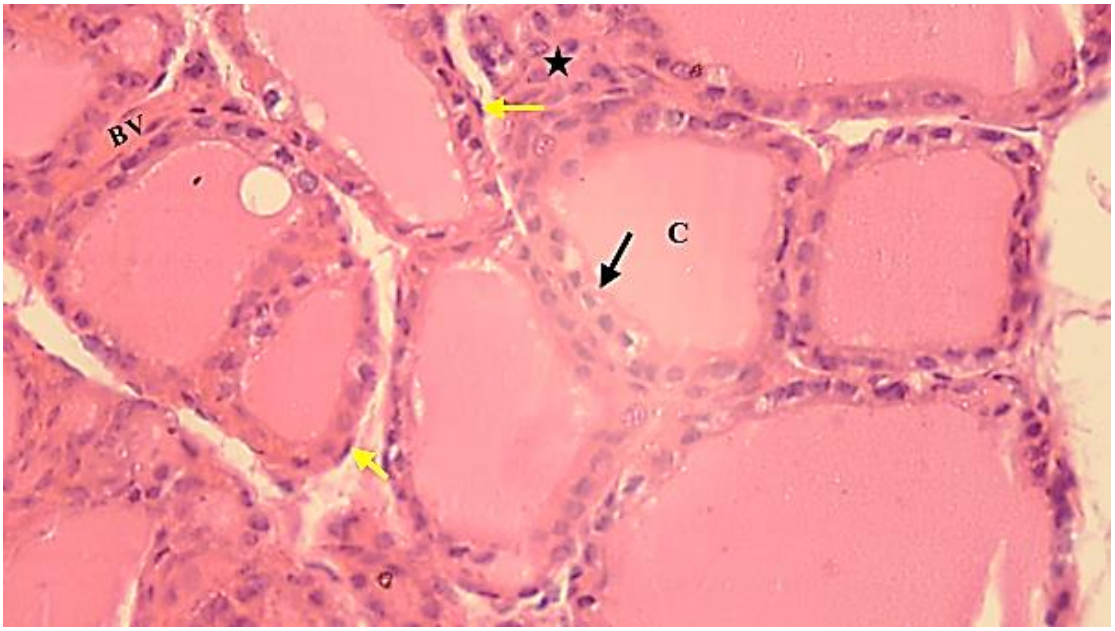

Fig. 3: A photomicrograph of a section of the thyroid gland of rats of GI showing variable-sized follicles filled with eosinophilic colloid with peripheral vacuolations **(C).** Each follicle is lined with a single layer of cuboidal thyrocytes **(black arrow)** that contain central rounded nuclei. Parafollicular cells are seen in between the follicles **(star).** Notice blood vessels in between the lobules **(BV).** Also, note the basement membrane surrounding the follicle **(yellow arrow).** **(H&E X 400**

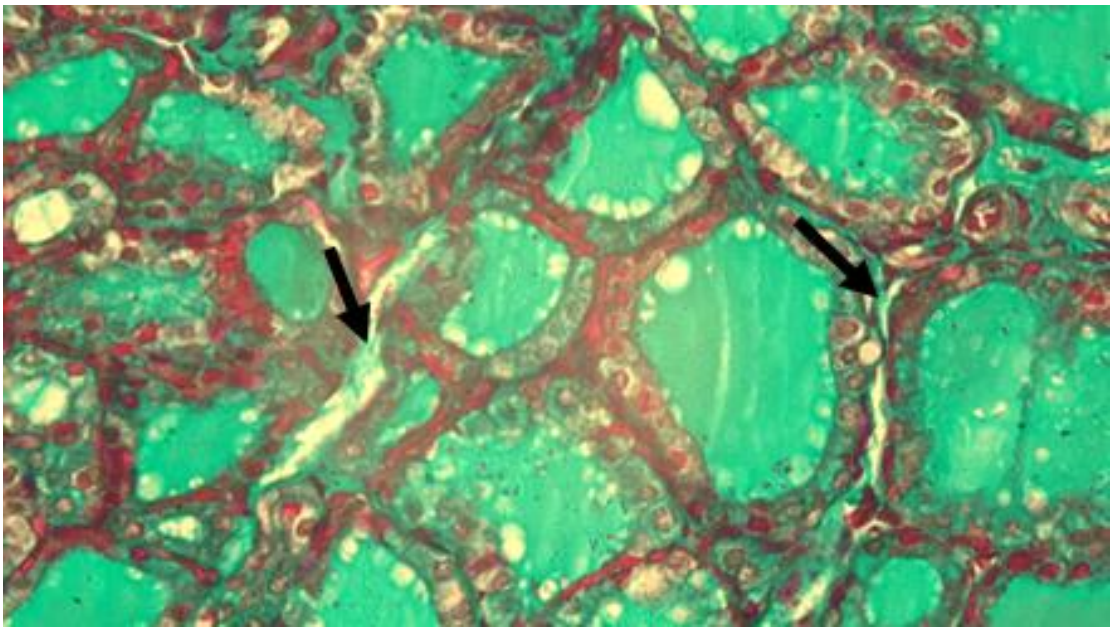

Fig. 4: A photomicrograph of a section of the thyroid gland of rats of GI showing the normal collagen fibers deposition **(arrow)** in the septa between the follicles. **(Masson 's trichrome X400)**

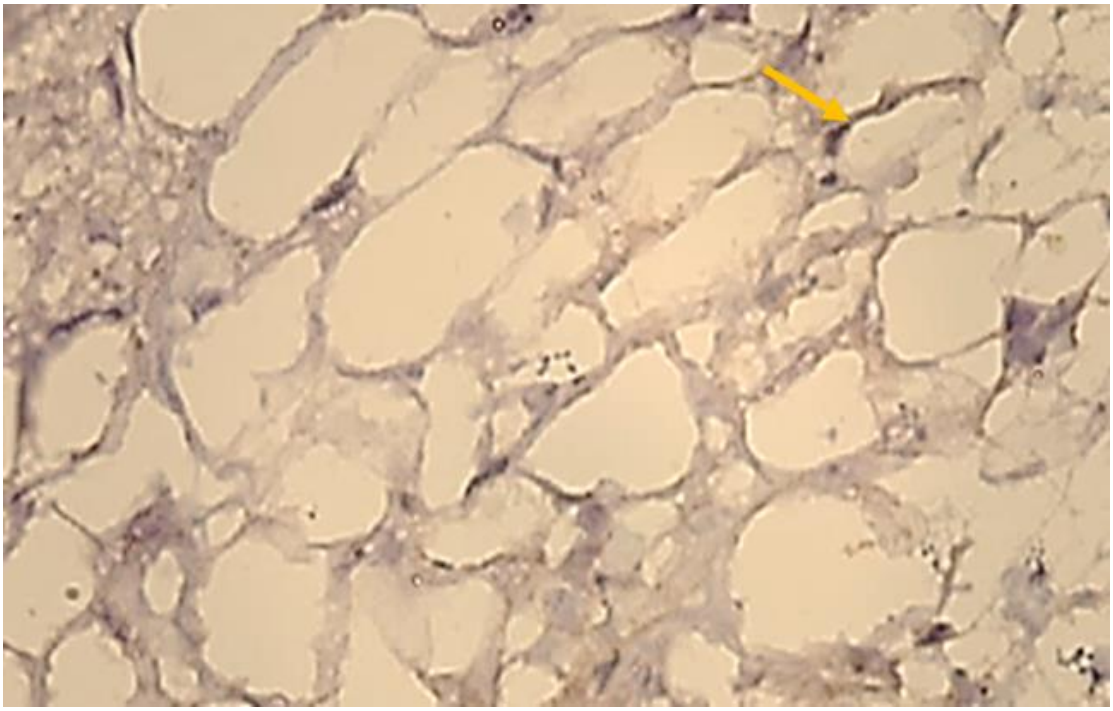

Fig. 5: A photomicrograph of a section of the thyroid gland of rats of GI showing weak positive immunoreactivity for caspase III in the nuclei and the cytoplasm of a few follicular cells **(yellow arrow). (Caspase III X400)**

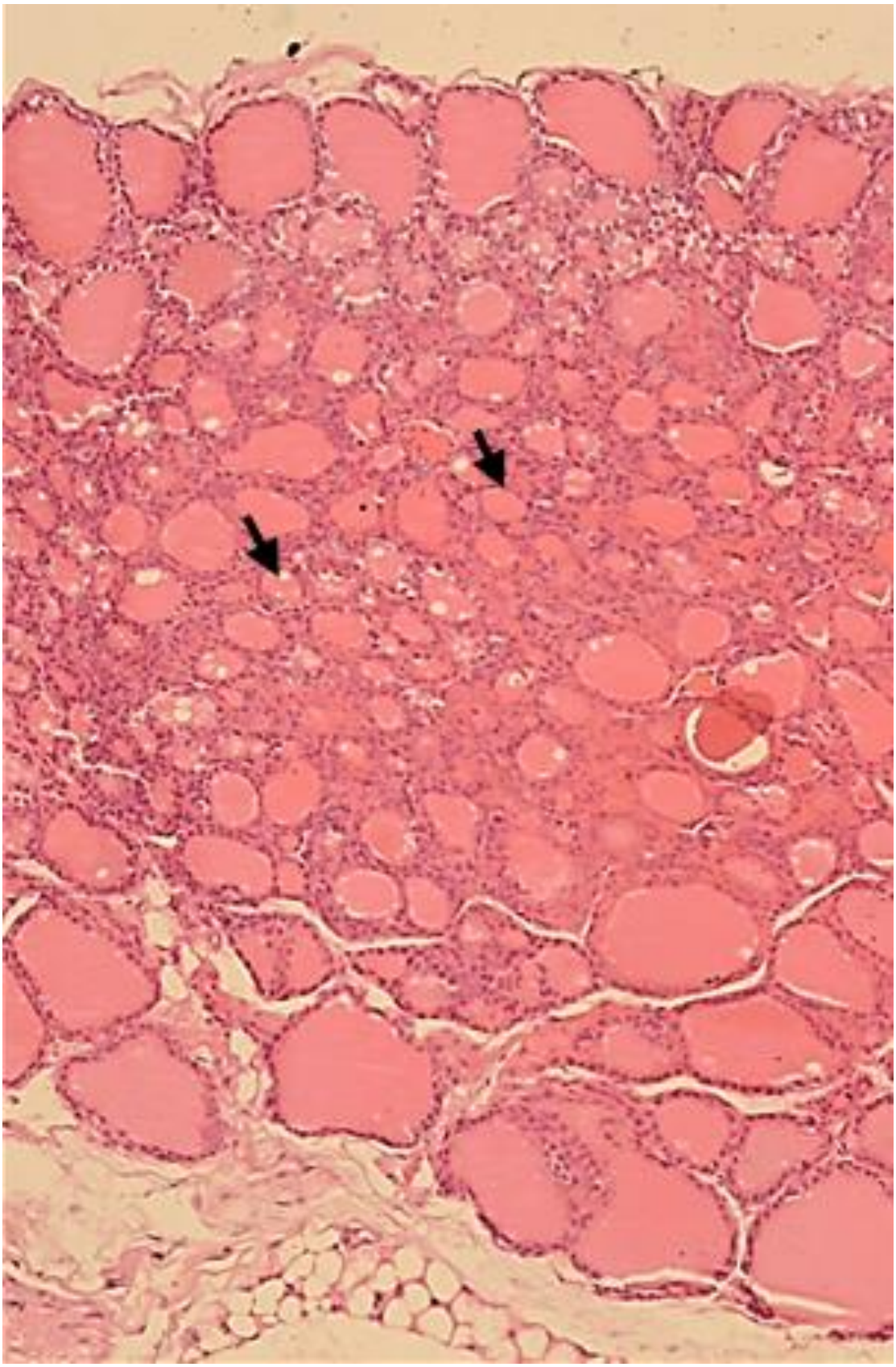

Fig. 6: A photomicrograph of a section of the thyroid gland of rats of GII showing loss of normal architecture of the thyroid gland. Notice the irregularly shaped and sized follicles with microcystic follicles **(arrow).** **(H&E X 100)**

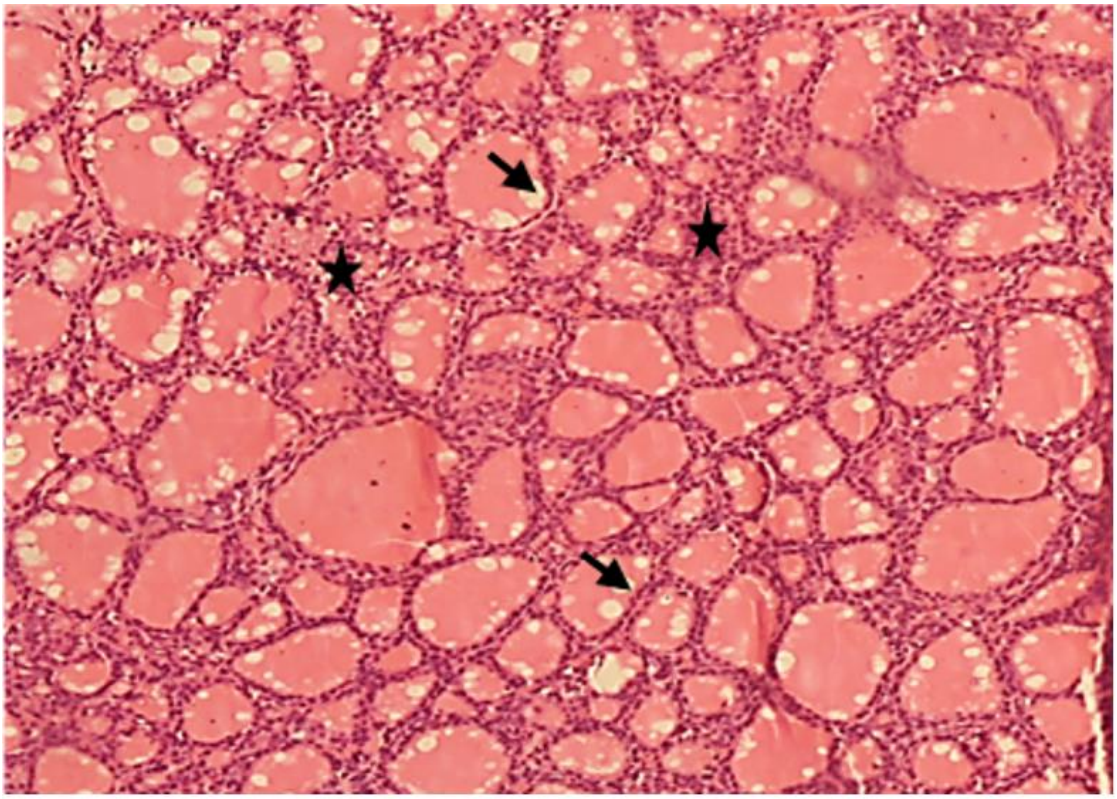

Fig. 7: A photomicrograph of a section of the thyroid gland of rats of GII showing the thyroid follicles filled with vacuolated colloid **(black arrow).** Notice the apparent increase in the number of parafollicular cells in between the thyroid follicles **(star).** **(H&E X 100)**

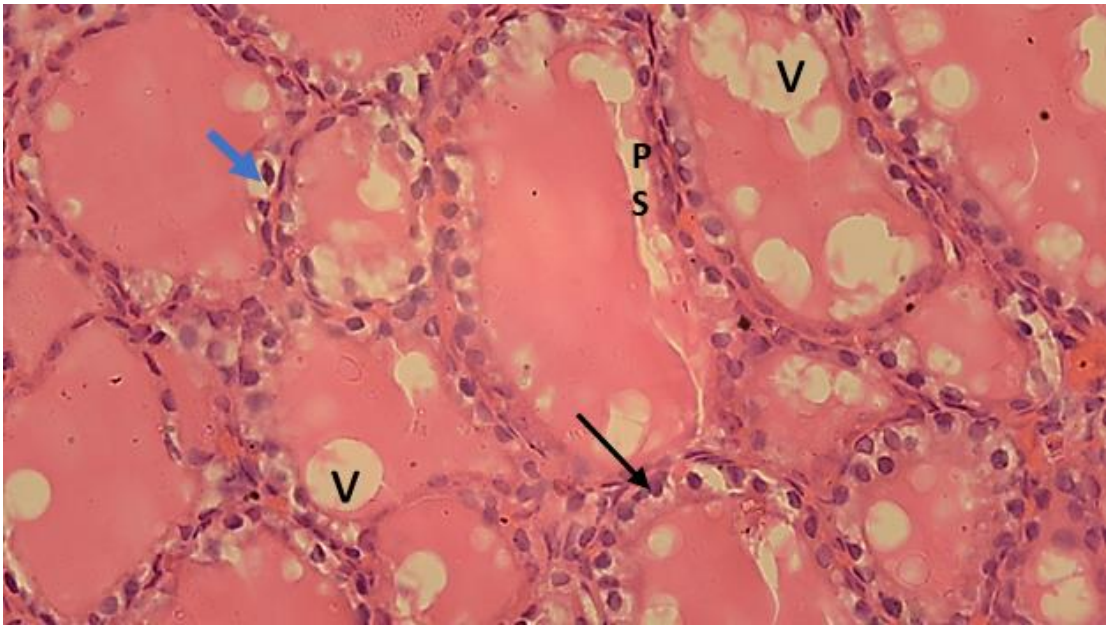

Fig. 8: A photomicrograph of a section of the thyroid gland of rats of GII showing the follicles are lined with columnar thyrocytes **(black arrow**) with vacuolated cytoplasm **(blue arrow**). The colloid of some follicles shows large-sized vacuolations **(V),** while others showed peripheral scalloping **(PS)**. **(H&E X 400)**

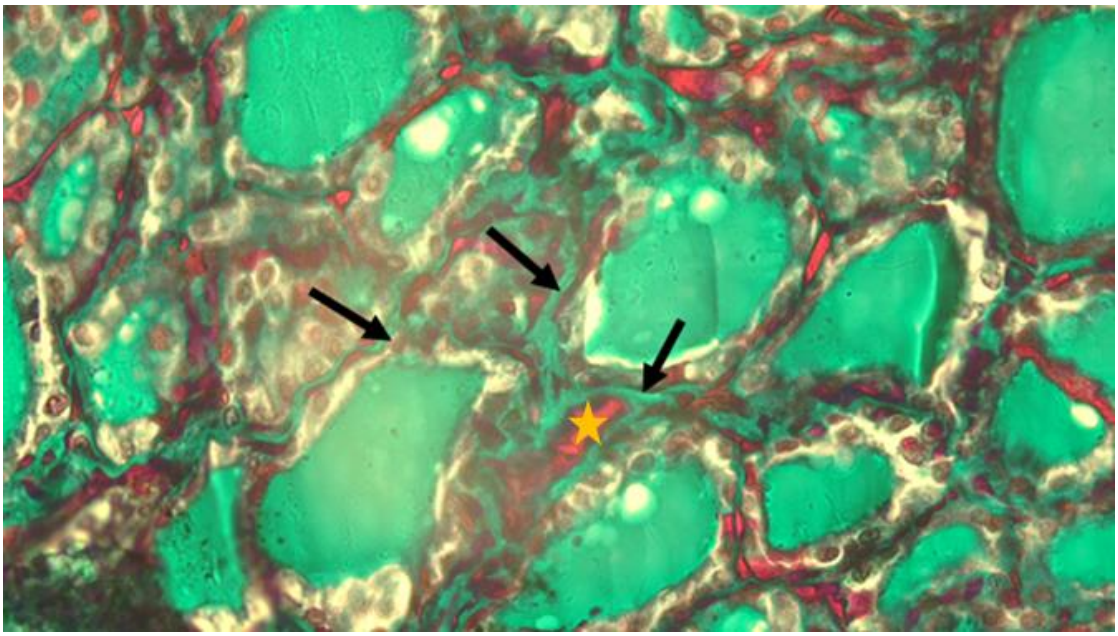

Fig. 9: A photomicrograph of a section of the thyroid gland of rats of GII showing a statistically highly significant increase in collagen fibers deposition in between the follicles compared to the control group **(arrows)**. Notice the interstitial congested blood vessels **(star).** **(Masson 's trichrome X400)**

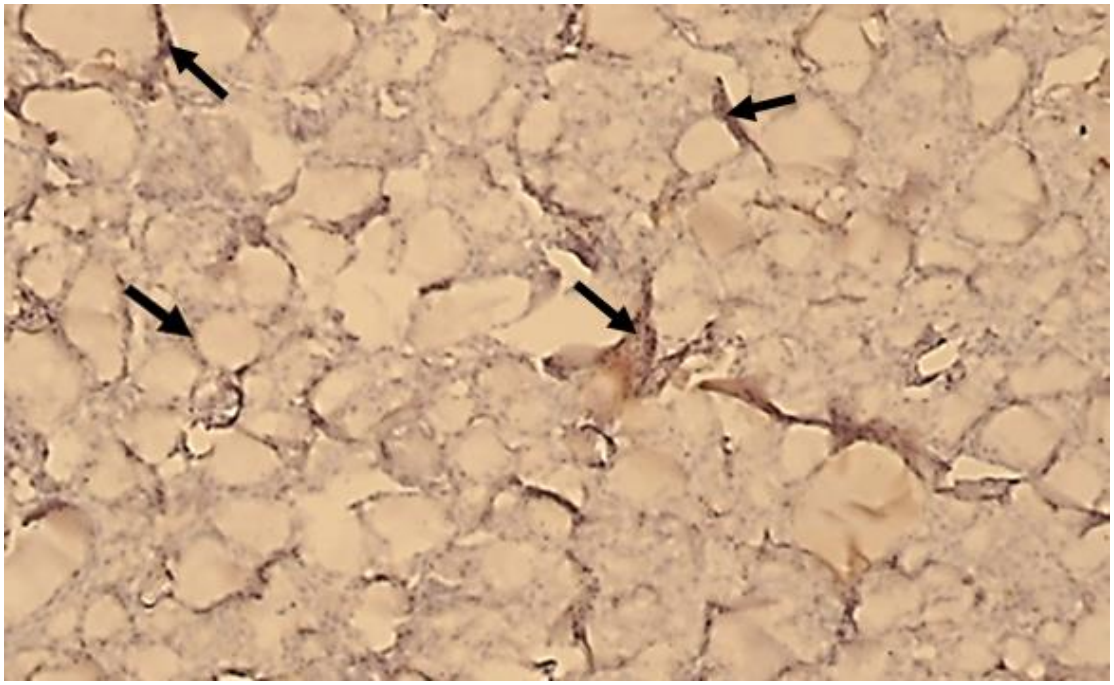

Fig. 10: A photomicrograph of a section of the thyroid gland of rats of GII showing a statistically significant increase in the nuclear and cytoplasmic immunoreactivity for caspase III in many follicular cells **(arrow).** **(Caspase III X400)**

Light microscopic examination of the thyroid glands of rats of group III (toxic dose treated group) showed severe disruption of the normal thyroid follicular architecture with loss of demarcation between the follicles. Some follicles showed papillary projection, while others had desquamated thyrocytes inside their lumina. Also, most of the follicles showed vacuolated or depleted colloids (Figs. 11 & 12). Some follicular thyrocytes showed hyperplasia, while others appeared with small deeply stained pyknotic nuclei with irregular outlines (Fig. 13). There was the widening of the interstitial

spaces in-between the follicles with the presence of thick-walled, congested and dilated blood vessels (Fig. 14). Also, there were areas of inflammatory cellular infiltration appeared in the interstitial spaces between some follicles (Fig. 15).

Masson's trichrome stained sections revealed a statistically highly significant increase in the distribution of collagen fibers deposition in between the follicles compared to the control group (Fig. 16) & (Table 2 & chart 2).

Immunohistochemically stained sections for caspase III showed a statistically highly significant nuclear and cytoplasmic immunoreactivity for caspase III in many follicular cells as compared to the control group (Fig. 17) & (Table 3 & chart 3).

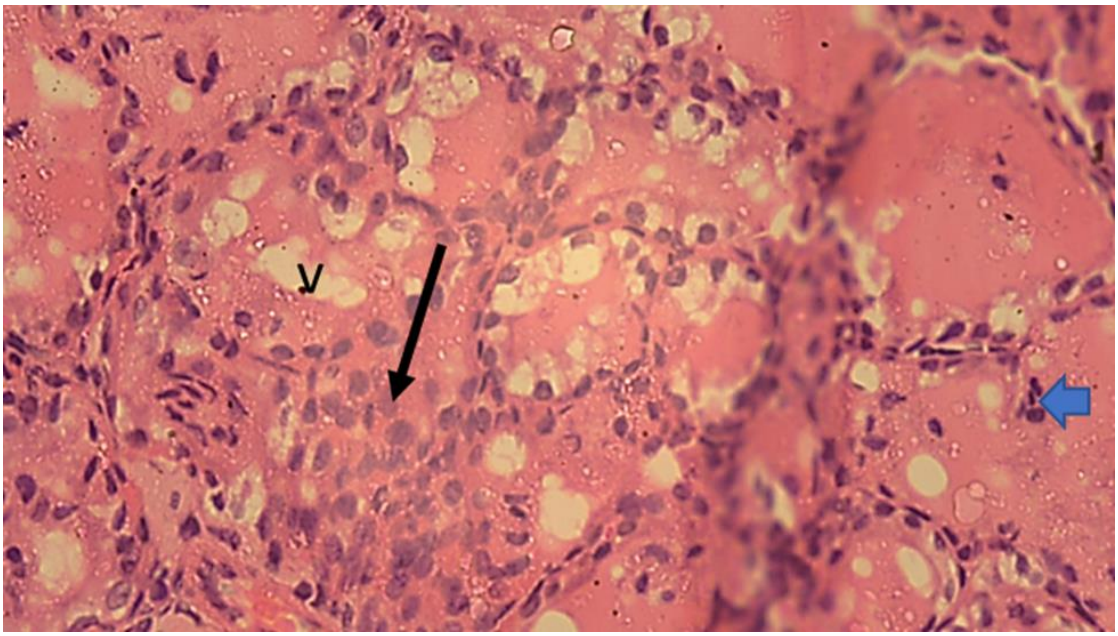

Fig. 11: A photomicrograph of a section of the thyroid gland of rats of GIII showing severe disruption of the normal thyroid follicular architecture, with loss of demarcation between the follicles. Some follicles show papillary projection inside the lumina **(Blue arrow)**. Other follicles have desquamated thyrocytes inside their lumina **(Black arrow).** Notice the vacuolated colloid in most of the follicles **(V).** **(H&E X 400)**

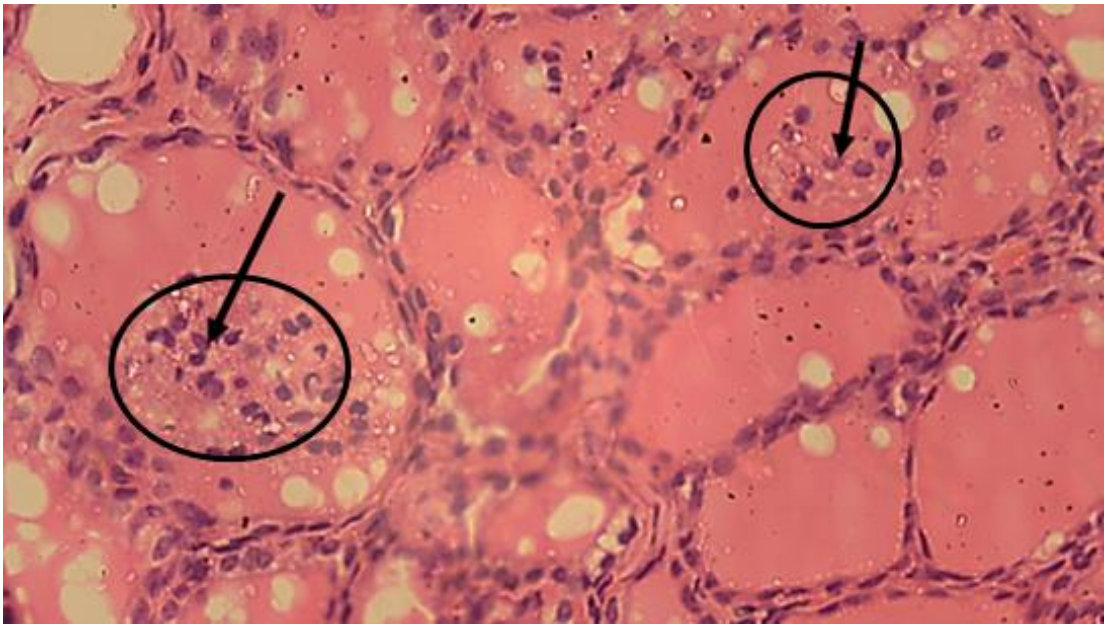

Fig. 12: A photomicrograph of a section of the thyroid gland of rats of GIII showing desquamated thyrocytes **(circle)** inside the lumina of some follicles having deeply stained pyknotic nuclei **(arrow).** **(H&E X400)**

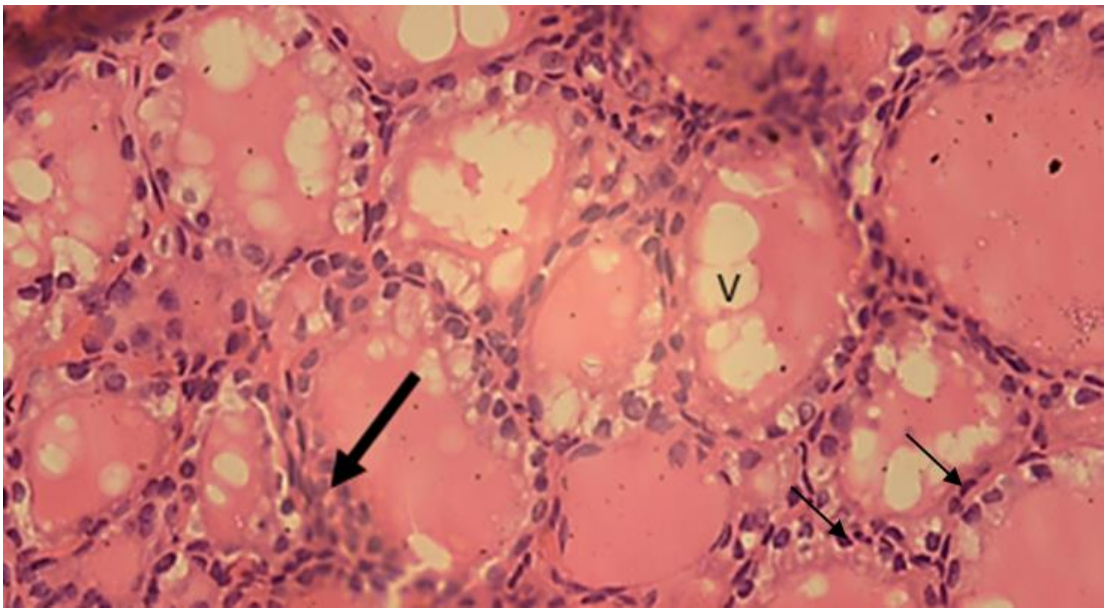

Fig. 13: A photomicrograph of a section of the thyroid gland of rats of GIII showing increased vacuolated colloid **(V)**. Some follicular thyrocytes showed hyperplasia **(thick arrow)**, while others appeared with small deeply stained pyknotic nuclei with irregular outlines **(thin arrow). (H&E X 400)**

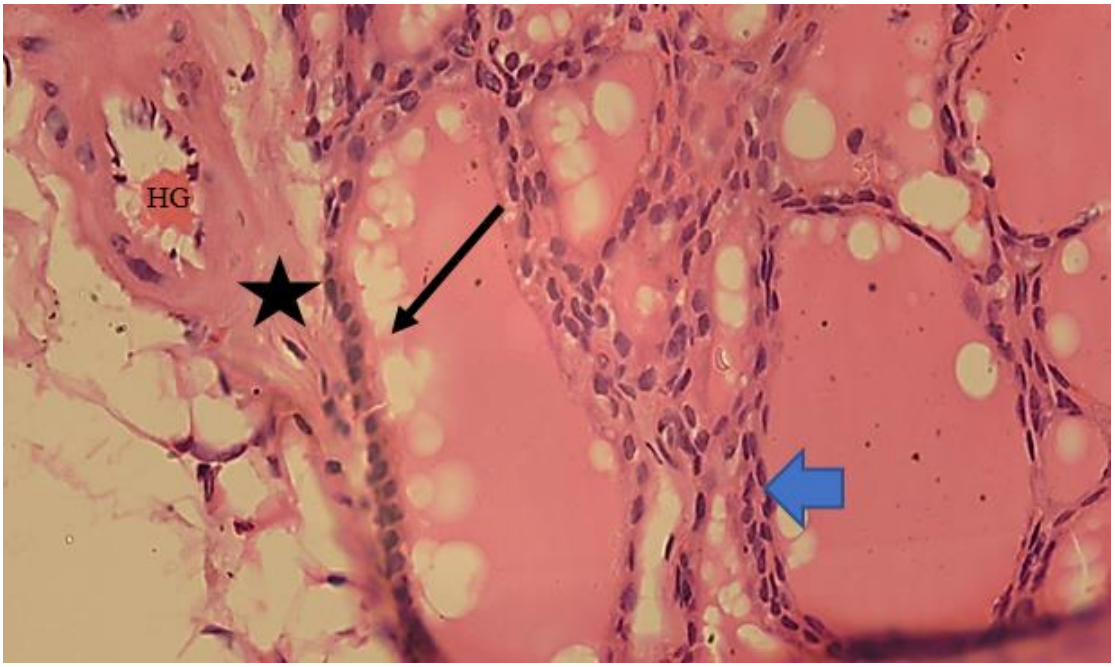

Fig. 14: A photomicrograph of a section of the thyroid gland of rats of GIII showing vacuolated colloid **(black arrow)**. The thyrocytes showed pyknotic nuclei **(Blue arrow).** Notice: the widening of the interstitial spaces in between the follicles and the presence of congested dilated and thick wall blood vessels **(BV)**. **(H&E X 400)**

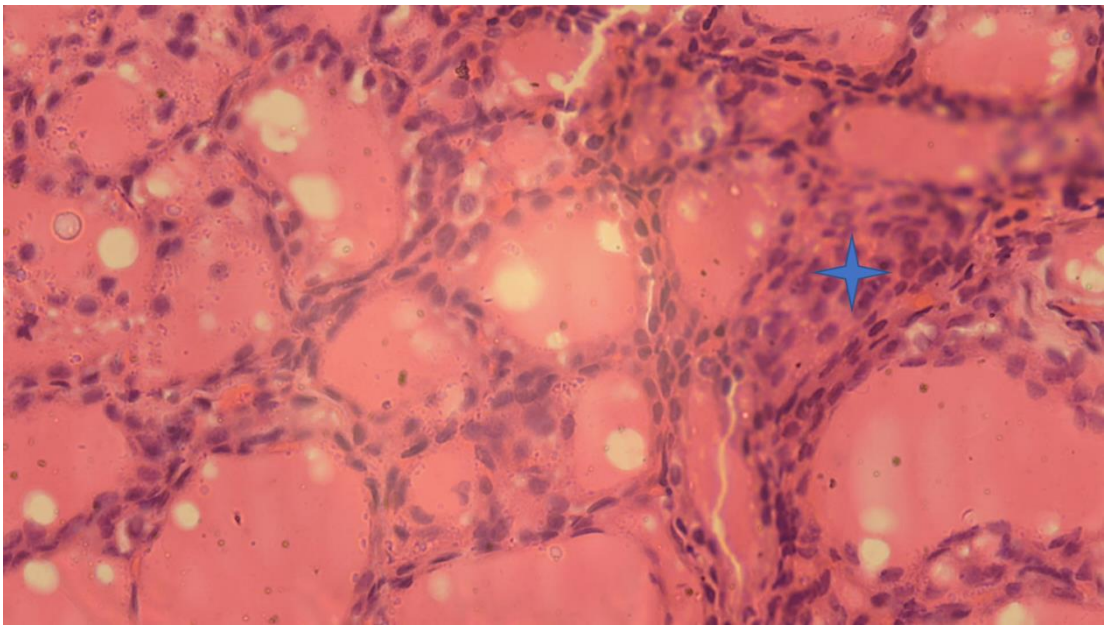

Fig. 15: A photomicrograph of a section of the thyroid gland of rats of GIII showing inflammatory cells infiltration within the interstitium **(star). (H&E X 400)**

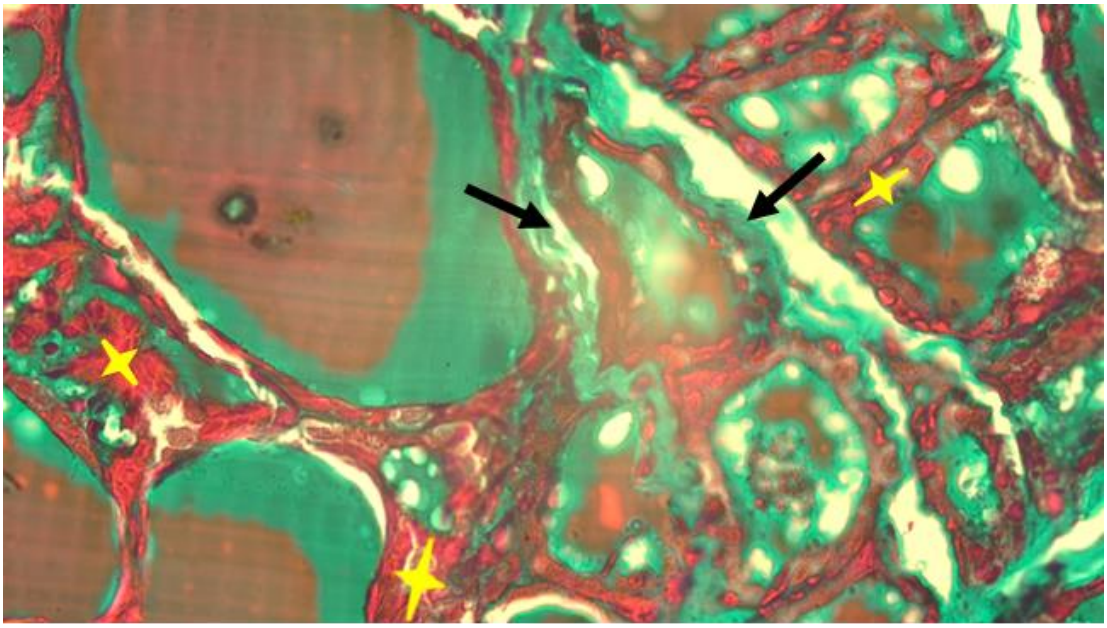

Fig. 16: A photomicrograph of a section of the thyroid gland of rats of GIII showing a statistically highly significant increase in collagen fibers deposition in between the follicles compared to the control group **(arrows)**. Notice the interstitial congested blood vessels **(star). (Masson 's trichrome X400)**

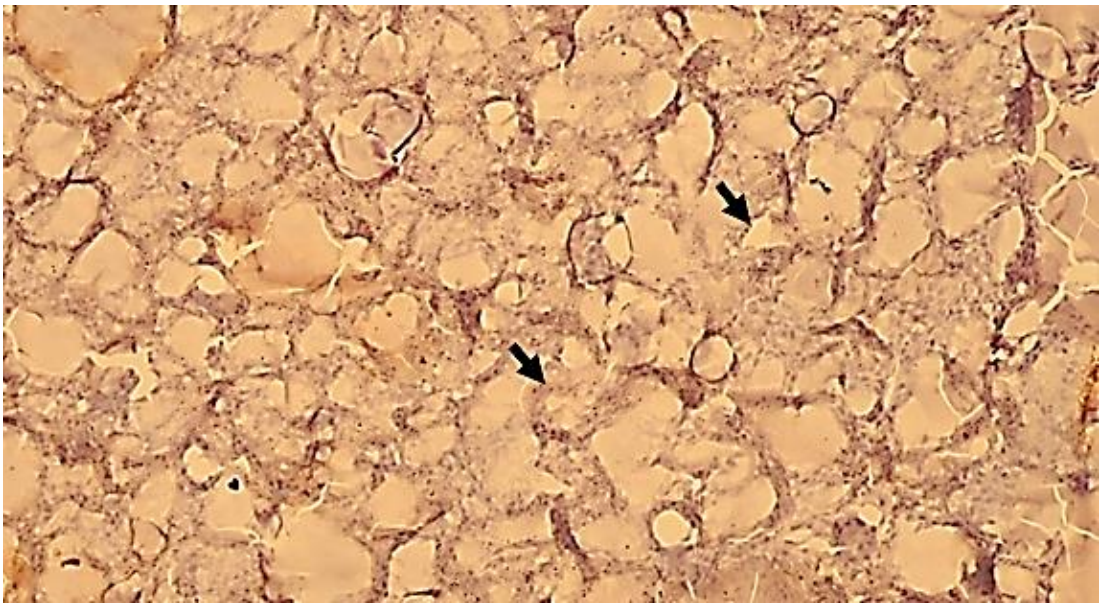

Fig. 17: A photomicrograph of a section of the thyroid gland of rats of GIII showing a statistically highly significant increase in the nuclear and cytoplasmic immunoreactivity for caspase III in many follicular cells **(arrow). (Caspase III X400)**

Morphometric Results and Statistical Analysis:

Statistical analysis of the area percentage of collagen deposition in between the thyroid follicles in Masson's trichrome stained sections revealed a highly significant increase in the collagen fibers deposition in between the thyroid follicles in both groups (II) and (III) in comparison to the control group (I).

Table 2: The mean area percentage of collagen deposition in between the thyroid follicles in all groups.

Groups	Mean	SD	P value
Control	0.82	0.148660687	
Treated group (II)	4.155714286	1.150548523	6.26936E-06*
Toxic group (III)	10.33571429	0.848152053	1.59704E-12*

*Probability (P) value was considered statistically significant if ≤ 0.05, and highly statistically significant if ≤ 0.001.
SD: Standard deviation

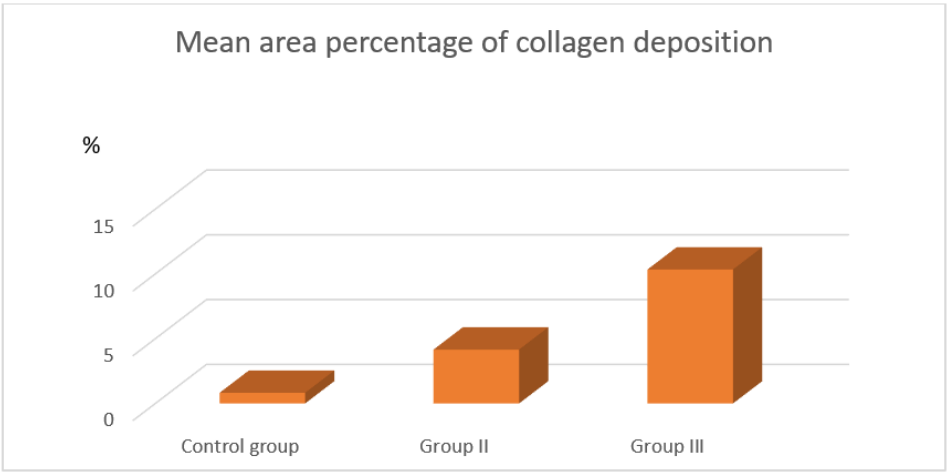

Chart 2: The mean area percentage of collagen fibers deposition in between the thyroid follicles in all groups

Mean Percentage of Caspase III Immunoreactivity:

Statistical analysis of the area percentage of caspase III immunoreactivity revealed a significant increase in the immunoreactivity for caspase III in group (II) in comparison to the control. Whereas there was a highly significant increase in the immunoreactivity for caspase III in group (III) as compared to the control.

Table 3: The Mean area percentage of caspase III immunoreactivity in all groups.

Groups	Mean	SD	P value
Control	0.28	0.068313005	
Treated group (II)	0.434285714	0.140220914	0.02250596*
Toxic group (III)	4.807142857	1.062163112	9.85886E-08*

*Probability (P) value was considered statistically significant if ≤ 0.05, and highly statistically significant if ≤ 0.001.
SD: Standard deviation

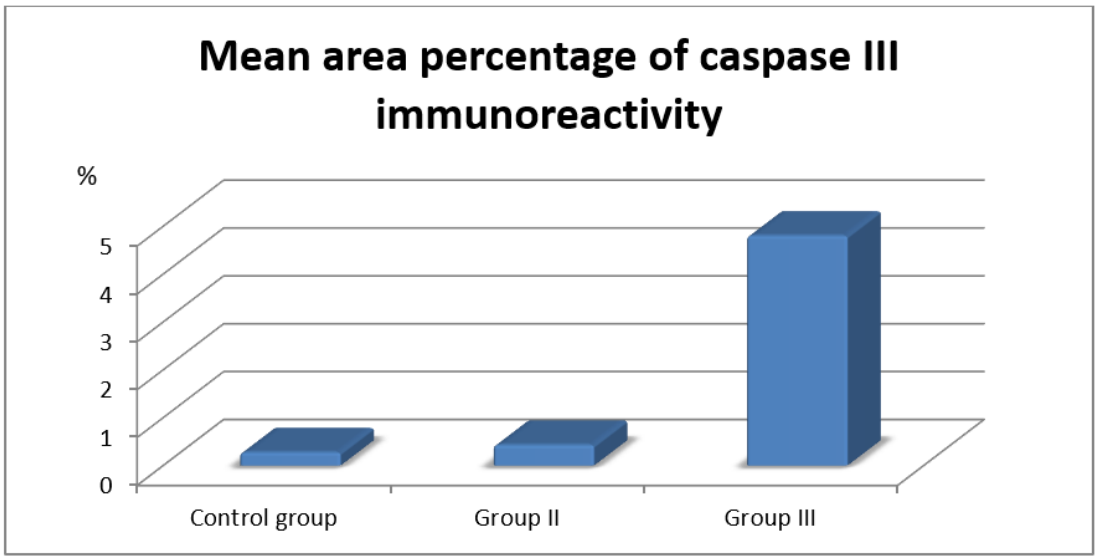

Chart 3: The Mean area percentage of caspase III immunoreactivity in all groups.

DISCUSSION

AMD is a potent antiarrhythmic drug that is widely used in tachyarrhythmias and to a lesser extent, in ischemic heart disease. It is an iodine-rich compound (37.3% of its molecular weight) (Maqdasy, *et al.*, 2019). So, it releases a 20 to 40 folds higher iodine level compared to the human body's daily requirements (Fonseca, *et al.*, 2022). The thyroid hormones; T3 and T4 have a significant impact on body metabolism, growth, and development and activity of the nervous system. Thus, any disturbance in their levels could adversely affect the metabolism of the whole body (Rajab, *et al.*, 2017). Therefore, AMD effects on thyroid functions had attracted considerable attention (Esmekaya, *et al.*, 2010).

Rodents and humans shared similarities in the histopathology of thyroid lesions. So, the rat model was relevant for the assessment of possible thyroid lesions in humans (Mahmoud and Solaiman, 2014). The oral intake of AMD was chosen in this study because it is similar to the conventional clinical situation in human cases (Mehta, *et al.*, 2008). In mammals, thyroid activity was commonly determined by the thyroid hormone secretion rate. Despite this, the histological examination of the gland was found to be the most sensitive parameter for the detection of any

factors that adversely affect thyroid function (Maynard and Downes, 2019).

The aim of the current study is to investigate the structural and biochemical changes of the thyroid gland of adult male albino rats after exposure to different doses of AMD.

As regards the biochemical results in the present study, there was a statistically significant increase in the level of T4 and a statistically significant decrease in the levels of free T3 and TSH in group II (AMD therapeutic dose-treated group), but in group III (AMD toxic dose-treated group), there was a statistically highly significant increase in in the level of T4 and a statistically highly significant decrease in the levels of free T3 and TSH. These results were in accordance with Ursella *et al.*, 2006, who found that AMD-induced thyrotoxicosis (AIT) could be diagnosed by increased serum T4 and decreased serum TSH concentration. Moreover, they added that AIT was usually associated with preferential secretion of T4 which was suggested by a high T4/T3 ratio.

The histological findings in the present study afforded evidence of the development of thyrotoxicosis which was marked in the AMD therapeutic dose-treated group (group II) and became severe in the AMD toxic dose-treated group (group III). There was a loss of the normal architecture of the thyroid gland in group (II), where most of the follicles appeared irregular in shape and size together with microcystic follicular changes. These findings agreed with Abdel Moaty, 2022, who found that the therapeutic dose of amiodarone could lead to irregularity in the shape and size of the thyroid acini with the presence of small cystic follicles filled with vacuolated colloid. Moreover, in our study, microscopic examination of thyroid tissue of group III (AMD toxic dose treated group) showed severe disruption of the histological architecture with loss of demarcation between the follicles. Some follicles showed papillary projection and desquamated thyrocytes inside their lumina together with vacuolated colloids. These findings were in agreement with Rasheed and Arsanyos, 2018.

In the present study, there was an apparent increase in the number of parafollicular cells in between the follicles and these findings were in agreement with Nakazawa et al., who reported an increase in parafollicular cells number following AMD administration (Nakazawa, *et al.*, 2008). Also, Martín-Lacave, *et al.*, 2009 reported that thyroid hyperactivity revealed the presence of enlarged parafollicular cells disseminated in small groups. These observations might point to the possibility of a relationship between the activity of parafollicular cells and the functional state of the thyroid gland.

In the present study, there was a widening of the interstitial spaces in between the follicles together with areas of inflammatory cell infiltration. Also, there was marked congestion and dilatation of blood vessels following AMD administration either in therapeutic or toxic doses. These findings were coincidental with Piga, *et al.*, 2008, who found that AMD could lead to degenerative and destructive follicular lesions with diffuse fibrous tissue lymphocytic infiltration in rats' thyroid glands.

Concerning nuclear changes following amiodarone administration in our study, many follicular cells revealed pyknotic nuclei indicating cell degeneration. It was noticed in group III more than in group II. This finding coincided with Mehta *et al.*, 2008, who noted pyknotic nuclei in the epithelium of many thyroid follicles in amiodarone-induced thyrotoxicosis patients. The iodine component of amiodarone was blamed to be the leading cause of this nuclear change through a p53-mechanism with subsequent oxidative stress (Vitale, *et al.*, 2000).

In the present work, there was a statistically highly significant increase in

collagen deposition in the thyroid gland in both AMD therapeutic and toxic doses treated groups (groups II & III). Also, El Sayed *et al.,* 2007 reported that amiodarone could induce degenerative and destructive follicular lesions and hemorrhage with focal fibrosis. Moreover, oxidative stress caused by AMD could activate transforming growth factor beta (TGF-β), which was considered the most effective cytokine in promoting fibrosis. TGF-β could cause fibrosis by stimulating fibroblasts to secrete matrix proteins (Koli, *et al.,* 2008).

In the present study, there was a statistically significant increase in caspase III immune expression in the follicular epithelial cells in groups II&III which denoted apoptotic cell death. It could be attributed to the direct toxic effect of AMD or its metabolites on the thyroid gland either directly or indirectly due to its high iodine content (Bogun, 2016). Diethyl AMD (DEA), which is considered the main AMD metabolite, was more cytotoxic on thyroid cells than AMD itself (Cappellani, *et al.,* 2020).

AMD might affect the thyroid gland and thyroid hormones metabolism in two ways; First by deactivating type-I-5′-deiodinase (5′-D), which is found in the liver to convert T4 to T3, leading to an increase in serum T4 and a decrease in serum T3 (Bogun, 2016). The second way might be attributed to the high iodine content of AMD, whereas iodine substrate from AMD could lead to excessive thyroid hormone synthesis and thyrotoxicosis, this phenomenon was known as the Jod-Basedow phenomenon (Eskes, *et al.,* 2012).

REFERENCES

Abdel Moaty, M. M. (2022): Dose-Related Amiodarone induced Thyrotoxicity in Adult Albino Rat and its Possible Reduction by Vitamin E: Histological and Immunohistochemical Study. *Journal of Medical Histology*, 6(4).

Aslan I., Aydin, I., and Aydin I. (2009): Functional Effects of Short-Term Treatment with Amiodarone on Thyroid Tissues of the Rabbit. *Biological Trace Element Research,* 133(2): 212-216.

Bancroft, J.D. and Gamble, M.N. (2002): Theory and Practice of Histological Techniques. 5th ed., Churchill-Livingstone, London, Edinburgh,175.

Benvenga, S., Tuccari, G., Ieni, A., and Vita, R. (2018): Thyroid Gland: Anatomy and Physiology. *Encyclopedia of Endocrine Diseases*, 4: 382-390.

Bogun, L. V. (2016): Amiodarone-induced thyroid dysfunction: Clinical case with literature review. *Journal of V. N. Karazin*, 32:627.

Branca, J. J., Lascialfari Bruschi, A., Pilia, A. M., Carrino, D., Guarnieri, G., Gulisano, M. and Paternostro, F. (2022): The Thyroid Gland: A Revision Study on Its Vascularization and Surgical Implications. *Medicina*, *58*(1), 137.

Cappellani, D., Papini, P., Pingitore, A., Tomisti, L., Mantuano, M., Di Certo, A. M. and Bogazzi, F. (2020): Comparison between total thyroidectomy and medical therapy for amiodarone -induced thyrotoxicosis. *The Journal of Clinical Endocrinology & Metabolism*, 105(1): 242-251.

Di Matola, T., (2000): Amiodarone Induces Cytochrome-C Release and Apoptosis through an Iodine-Independent Mechanism. *Journal of Clinical Endocrinology & Metabolism*, 85(11): 4323-4330.

El Sayed, O. A., Gawish, S. E., Aweida, G. and Auda, E. A. (2007): Histopathological and biochemical toxic effect of amiodarone on thyroid gland in albino rat. *The Egyptian*

Journal of Hospital Medicine, 29(1), 463-474.

Epstein, A.E., Olshansky, B., Naccarelli, G.V, et al. (2016): Practical management guide for clinicians who treat patients with amiodarone. *American Journal of Medicine,* 129:468–475.

Eskes, S.A., Endert, E. and Fliers, E. (2012): Treatment of amiodarone -induced thyrotoxicosis type 2: a randomized clinical trial. *Journal of Clinical Endocrinology and Metabolism*, 97(2): 499-506.

Eşmekaya, M.A., Seyhan, N. and Ömeroğlu, S. (2010): Pulse modulated 900 MHz radiation induces hypothyroidism and apoptosis in thyroid cells: a light, electron microscopy and immunohistochemical study. *International journal of radiation biology*, 86(12): 1106-1116.

Fischer, A.J., Enders, D., Eckardt, L., Köbe, J., Wasmer, K., Breithardt, G., De Torres Alba, F., Kaleschke, G., Baumgartner, H. and Diller, G.P. (2022): Thyroid dysfunction under amiodarone in patients with and without congenital heart disease: results of a nationwide analysis. *Journal of Clinical Medicine,* 11(7): 2027.

Fonseca, M., Ferreira, M., Paulo, J. and Neves, Z. (2022): A Refractory Case of Amiodarone Thyrotoxicosis. *The Cureus Journal of Medical Science*, 14(8).

Jabrocka-Hybel, A., Bednarczuk, T., Bartalena, L., *et al.* (2015): Amiodarone and the thyroid. *Endokrynologia Polska*, 66(2): 176-86.

January, C.T., Wann, L.S., Alpert, J.S., *et al.* (2014): 2014 AHA /ACC/HRS guideline for the management of patients with atrial fibrillation: executive summary: a report of the American College of Cardiology/American Heart Association Task Force on practice guidelines and the Heart Rhythm Society. *Circulation,* 130: 2071-2104.

Koli, K., Myllarniemi, M., Keski-Oja, J., et al., (2008): Transforming growth factor-bactivation in the lung: focus on fibrosis andreactive oxygen species. *Antioxid Redox Signal*, 10: 333-342.

Mahmoud, S.A. and Solaiman, A.A. (2014): Light and electron microscopic study of thyroid follicular cells in adult albino rats following green tea administration. *Egyptian Journal of Histology,* 37 (2) :417-427.

Maqdasy, S., Benichou, T., Dallel, S., et al., (2019): Issues in amiodarone -induced thyrotoxicosis: Update and review of the literature. *Annales d'endocrinologie,* 80(1): 54-60.

Martín-Lacave I., Borrero MJ., Utrilla JC., Fernández-Santos JM. et al. (2009): C-cells evolve at the same rhythm as follicular cells when thyroidal status changes in rats. *Journal of Anatomy*, 214:301-309.

Maynard, R.L. and Downes, N. (2019): Anatomy and Histology of the Laboratory Rat in toxicology and biomedical research. Chapter 16 (endocrine glands). Academic Press. P: 188-190.

Mehta, A.N., Vallera, R.D., Tate, C.R., et al., (2008): Total thyroidectomy for medically refractory amiodarone-induced thyrotoxicosis. *Proceedings (Baylor University. Medical Center)*, 21(4): 3825.

Nafrialdi, N., Kurniawan, T.G., Setiawati, A. and Makmun,

L.H. (2014): QT interval prolongation associated with amiodarone use in Cipto Mangunkusumo Hospital, Jakarta. *Acta Medica Indonesiana,* 46: 292–297.

Nakazawa T., Murata S.-I., Kondo T., et al. (2008): Histopathology of the thyroid in amiodarone-induced hypothyroidism. *Pathology International,* 58(1) : 55-58.

Piga, M., Cocco, M.C., Serra, A., et al. (2008): The usefulness of 99mTc-sestaMIBI thyroid scan in the differential diagnosis and management of amiodarone -induced thyrotoxicosis. *European Journal of Endocrinology*, 159:423–429.

Rajab, N.M., Ukropina, M. and Cakic-Milosevic, M. (2017): Histological and ultrastructural alterations of the rat thyroid gland after short-term treatment with high doses of thyroid hormones. *Saudi Journal of Biological Sciences*, 24(6):1117-1125.

Rasheed, R. and & Arsanyos, S. (2018): Vitamin e ameliorates the toxic effect of amiodarone on thyroid gland in rats: a histological and ultrastructural study. *Journal of Medical Histology*, 2(1), 57-68.

Sawilowsky, S. (2005): Misconceptions Leading to Choosing the t Test Over the Wilcoxon Mann-Whitney Test for Shift in Location Parameter. *Journal of Modern Applied Statistical Methods*, 4(2): 598-600.

Singh, R. (2020): Surgical Anatomy of Thyroid Gland. A Comprehensive Review. *Basic Sciences of Medicine*, 9(1): 10-14.

Talat, A., Khan, A.A., Nasreen, S. and Wass, J.A. (2019): Thyroid Screening During Early Pregnancy and the Need for Trimester Specific Reference Ranges: A Cross-Sectional Study in Lahore, Pakistan. *The Cureus Journal of Medical Science*,11(9): e5661.

Ursella, S.; Testa, A., Mazzone, M. et al. (2006): Amiodarone-induced thyroid dysfunction in clinical practice. *European Review for Medical and Pharmacological Sciences*, 10 (5): 269-278.

Vitale, M., Di Matola, T., D'Ascoli, F., Salzano, S., Bogazzi, F., Fenzi, G., Martino, E. and Rossi, G. (2000): Iodide excess induces apoptosis in thyroid cells through a p53-independent mechanism involving oxidative stress. *Endocrinology*, 141(2): 598-605.

Zidan, R. (2011): Effect of long-term administration of amiodarone on rat lung and the possible protective role of vitamin E. *The Egyptian Journal of Histology*, 34(1): 117-128.